

Buckling problem of sandwich rectangular plates consisting of polymer-based nanocomposite layers under compressive load

C. Bozkurt¹, H. Dilmac², A.H. Sofiyev^{3,4*}

¹*Suleyman Demirel University, Graduate School of Natural and Applied Sciences, Isparta, Turkey*

²*Department of Civil Engineering Suleyman Demirel University, Isparta, Turkey*

³*Department of Mathematics, Istanbul Ticaret University, Beyoglu 34445, Istanbul, Turkey*

⁴*Scientific Research Center, Odlar Yurdu University, Baku AZ1012, Azerbaijan*

email: aavey@ticaret.edu.tr

Abstract

In this work, buckling problem of polymer-based sandwich rectangular plates with uniform and heterogeneous (HT) reinforced layers subjected to uniaxial compressive load is investigated. First, mechanical properties of each layer of sandwich rectangular plates consisting of polymer nanocomposites are modeled according to the extended mixture rule. After the basic relations of sandwich plates consisting of polymer-based nanocomposite layers are constructed, governing equations are derived based on the assumptions of classical plate theory (CPT). The governing equations under simply supported boundary conditions are solved and analytical expression is found for the critical compressive load. The numerical calculations are made for the minimum values of uniaxial critical load loads for different volume fraction ratios in the layers, four different carbon nanotube (CNT) patterns in the layers, layer alignment and various plate sizes, and these calculations are interpreted, and the generalization of the interpretations constitutes the conclusion.

Keywords: Carbon nanotubes, nanocomposite, sandwich plates, buckling, compressive load.

PACS numbers: 62.23.Pq, 62.25.-g

Received:
12 April 2025

Revised:
30 April 2025

Accepted:
14 May 2025

Published:
26 May 2025

1. Introduction

In the field of nanotechnology, one of the most popular topics for current research and development is polymer-based nanocomposites, and the research area covers a wide range of topics. Polymer-based nanocomposites have recently become a focus of interest for the defense industry and other high-tech industries due to their extraordinary properties, both as carrier elements and intermediate elements. CNTs, one of the components of the nanocomposite, have proven to be an ideal choice as fillers for both structural and functional applications due to their extraordinary properties, such as providing an extraordinary improvement in the properties of the polymer matrix, the main component of the nanocomposite [1-3]. Nanocomposites have significant advantages over traditional materials, such as very high tensile and flexural strength, light weight, high elasticity modulus and wear resistance, high thermal stability, flame retardant properties, improved specific strength and hardness, improved fracture toughness, thermal shock resistance and significant electrical conductivity. These advantages enable the use of nanocomposites in sandwich structures as

well as in different structural systems [4-5]. The first study on the stability of functionally graded nanocomposite structural elements was related to single-layer plates and was proposed in the study of Shen [6]. After this study, many research on the stability of single-layer functionally graded nanocomposite structural elements in different conditions [7-11].

One of the most economical ways to obtain satisfactory mechanical properties of structural elements is to perform hybridizations involving the use of more than one composite material. One type of hybrid composites is sandwich structures, which consist of two relatively rigid face layers and a soft core [12].

The most important disadvantage of sandwich structural elements consisting of traditional composites is the delamination of the layers due to the difference in mechanical properties. The discovery of new generation composites plays an important role in eliminating these negativities. In recent years, nanocomposite layers have begun to be frequently used in sandwich systems in various areas of modern technology. In terms of the reliability of these applications, there is a need to investigate the buckling behavior of triple systems containing nanocomposite layers, especially triple-layer plate systems. The number of publications on the buckling problem of sandwich or multi-layer nanocomposite plates is quite limited. Lei et al. [13] studied the buckling behavior of functionally graded layered composite plates reinforced with carbon nanotubes was investigated using the meshless kp-Ritz method. Long and Tung [14] investigated the buckling and post-buckling behavior of sandwich plates reinforced with single-walled carbon nanotubes resting on elastic foundations and subjected to uniform temperature increase. Tan et al. [15] proposed novel sandwich composite shell structures in nonlinear geometric and dynamic analyses. Sofiyev and Avey [16] presented modeling and applications of laminated nanocomposite structural elements in thermal environments. Sofiyev et al. [17] proposed a mathematical approach to the buckling problem of axially loaded laminated nanocomposite cylindrical shells in various environments.

The literature review shows that the buckling behavior of sandwich plates consisting of nanocomposites under the effect of in-plane uniaxial and biaxial compressive forces has not been investigated in detail. Since accurate and effective buckling analysis of sandwich plates containing nanocomposite layers is of critical importance to achieve optimized and reliable designs, this issue will be discussed in detail in this study.

2. Formulation of the problem

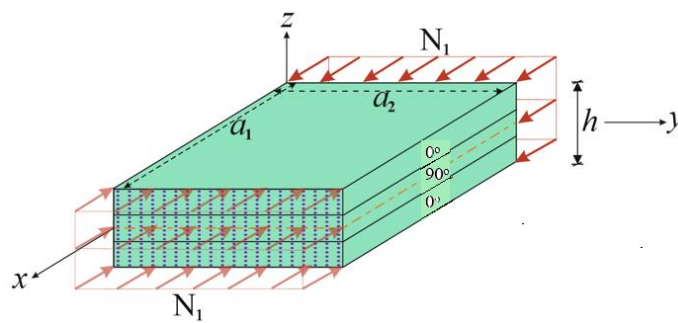


Figure 1. A sandwich rectangular plate containing three nanocomposite layers under uniaxial compressive load and the coordinate system

A sandwich rectangular plate with $(0^\circ/90^\circ/0^\circ)$ arrangement containing nanocomposite layers presented in figure 1 that is under unidirectional compressive load, the length and width are a_1 and a_2 , the thickness of each layer is h_0 and the total thickness of the sandwich plate is h . The compressive load N_1 acts in the direction of the Ox axis. It is assumed that the layers are perfectly and rigidly bonded to each other and that the layers do not break apart when a deformation occurs. The rectangular sandwich plate has a continuous heterogeneous orthotropic structure with pieces, each layer consists of a carbon nanotube reinforced polymer

matrix and has the same carbon nanotube volume fraction. The $Oxyz$ coordinate system is in the back left corner of the origin rectangular sandwich plate and in the reference plane of the middle layer, the Ox axis is in the longitudinal direction, the Oy axis is in the transverse direction and the Oz axis is perpendicular to the reference plane. The three perpendicular displacements of any point in the reference plane of the three-layer rectangular plate are shown as U , V and W , respectively.

In this study, multi-scale modeling of CNTs and polymer matrix is performed. It is known that the effective material properties of nanocomposites largely depend on the structure of CNTs [2-5]. It is well known that to estimate the effective material properties of multilayered and specially sandwich nanocomposite rectangular plates layers, the extended Voigt model is used [6-11], where the CNT efficiency parameters are defined to take into account the size dependence of the resulting nanostructures. According to this rule, the effective Young's modulus and shear modulus of each nanocomposite layer can be estimated as follows [13, 17]:

$$E_{11NC}^{(k)} = \eta_1^{(k)} V_{zcnt}^{(k)} E_{11cnt}^{(k)} + V_p^{(k)} E_p^{(k)}, \frac{\eta_2^{(k)}}{E_{22NC}^{(k)}} = \frac{V_{zcnt}^{(k)}}{E_{22cnt}^{(k)}} + \frac{V_p^{(k)}}{E_p^{(k)}}, \frac{\eta_3^{(k)}}{G_{12NC}^{(k)}} = \frac{V_{zcnt}^{(k)}}{G_{12cnt}^{(k)}} + \frac{V_p^{(k)}}{G_p^{(k)}} \quad (1)$$

where $E_{ii}^{(k)}, G_{12}^{(k)}$ ($i = 1,2, k = 1,2,3$) and $E_p^{(k)}, G_p^{(k)}$ are the Young and shear modulus of elasticity of the k -th layer CNT and polymer, respectively, of the sandwich rectangular plate. $V_{cnt}^{(k)}$ and $V_p^{(k)}$ represent the volume fractions of the k -th layer CNT and the polymer matrix, respectively, and the following relation satisfied: $V_{cnt}^{(k)} + V_p^{(k)} = 1$.

To account for the small-scale effect, the efficiency parameters of the CN, denoted by $\eta_j^{(k)}$ ($j = 1,2,3$), are obtained by matching the Young moduli of the nanocomposite layer estimated from the extended Voigt models with the values found from the molecular dynamics simulations, as previously presented in [3].

Since the Poisson's ratio and mass density of the nanocomposite layer vary within a small range, the Poisson's ratio and mass density of the components can be easily expressed according to the traditional mixing rule as:

$$\nu_{12}^{(k)} = V_{cnt}^{(k)} \nu_{12cnt}^{(k)} + V_p^{(k)} \nu_p^{(k)}, \rho_t^{(k)} = V_{cnt}^{(k)} \rho_{cnt}^{(k)} + V_p^{(k)} \rho_p^{(k)} \quad (2)$$

The mathematical models characterizing the volume fraction distributions of the k -th layer CNT are given as follows [6, 13, 16]:

$$V_{cnt}^{(k)} = V_{cnt}^{*(k)}(U) \quad (3)$$

$$V_{zcnt}^{(k)} = 2(0.5 - \bar{z})V_{cnt}^{*(k)}(V) \quad (4)$$

$$V_{zcnt}^{(k)} = 2(1 - 2|\bar{z}|)V_{cnt}^{*(k)}(O) \quad (5)$$

$$V_{zcnt}^{(k)} = 4|\bar{z}|V_{cnt}^{*(k)}(X) \quad (6)$$

Pre-buckling properties of sandwich HT-nanocomposite rectangular plates presented in figure 1 can be expressed as follows and indicated by superscript "0" [18, 19]:

$$N_{11}^0 = -N_1, N_{22}^0 = N_{12}^0 = 0 \quad (7)$$

where $N_{11}^0, N_{22}^0, N_{12}^0$ are the membrane forces for the zero initial moment condition.

The dependence between the $N_{ij}(i, j = 1, 2)$ force components and the Airy stress function (F) is defined as follows [18, 19]:

$$(N_{11}, N_{22}, N_{12}) = \left(h \frac{\partial^2 F}{\partial y^2}, h \frac{\partial^2 F}{\partial x^2}, -h \frac{\partial^2 F}{\partial x \partial y} \right) \quad (8)$$

3. Basic equations

Within the framework of classical plate theory, the stress-strain relationships in each layer of sandwich rectangular plates consisting of heterogeneous nanocomposite layers are defined as follows [11, 16]:

$$\begin{bmatrix} \sigma_{11}^{(k)} \\ \sigma_{22}^{(k)} \\ \sigma_{12}^{(k)} \end{bmatrix} = \begin{bmatrix} \bar{E}_{11NC}^{(k)} & \bar{E}_{12NC}^{(k)} & 0 \\ \bar{E}_{21NC}^{(k)} & \bar{E}_{22NC}^{(k)} & 0 \\ 0 & 0 & \bar{E}_{66NC}^{(k)} \end{bmatrix} \begin{bmatrix} \varepsilon_{11}^0 - z \frac{\partial^2 W}{\partial x^2} \\ \varepsilon_{22}^0 - z \frac{\partial^2 W}{\partial y^2} \\ \varepsilon_{12}^0 - 2z \frac{\partial^2 W}{\partial x \partial y} \end{bmatrix} \quad (9)$$

where, $\sigma_{ij}^{(k)}(i, j = 1, 2)$ are the stress components in the k th layer, $\varepsilon_{ij}^0(i, j = 1, 2)$ are the strain components in the mid-plane of the three-layer rectangular plate consisting of nanocomposite layers and $\bar{E}_{ijNC}^{(k)}(i, j = 1, 2, 6)$ are the coefficients defining the elastic properties of the layers consisting of nanocomposites are expressed as follows:

$$\begin{aligned} \bar{E}_{11NC}^{(k)} &= \frac{E_{11NC}^{(k)}}{1 - \left(\nu_{12NC}^{(k)}\right)^2}, \bar{E}_{12NC}^{(k)} = \frac{\nu_{21NC}^{(k)} E_{11NC}^{(k)}}{1 - \left(\nu_{12NC}^{(k)}\right)^2} = \frac{\nu_{12NC}^{(k)} E_{22NC}^{(k)}}{1 - \left(\nu_{12NC}^{(k)}\right)^2} = \bar{E}_{21NC}^{(k)}, \\ \bar{E}_{22NC}^{(k)} &= \frac{E_{22NC}^{(k)}}{1 - \left(\nu_{12NC}^{(k)}\right)^2}, \bar{E}_{66NC}^{(k)} = \frac{G_{12NC}^{(k)}}{2(1 + \nu_{12NC}^{(k)})} \end{aligned} \quad (10)$$

The forces and moments are defined as follows [18, 19]:

$$(N_{ij}, M_{ij}) = \sum_{k=1}^3 \int_{z_{k-1}}^{z_k} \sigma_{ij}^{(k)}(1, z) dz, (i, j = 1, 2, 6) \quad (11)$$

where

$$-\frac{h}{2} + \frac{(k-1)h}{N} \leq z \leq -\frac{h}{2} + \frac{kh}{N} \quad (12)$$

By using the relationships from (9) to (11), the governing equations for sandwich heterogeneous plates composed within CPT are obtained as follows:

$$\begin{aligned} R_{12} \frac{\partial^4 F}{\partial x^4} + (R_{11} + R_{22} - 2R_{31}) \frac{\partial^4 F}{\partial x^2 \partial y^2} + R_{21} \frac{\partial^4 F}{\partial y^4} - R_{13} \frac{\partial^4 W}{\partial x^4} - \\ - (R_{14} + R_{23} + 2R_{32}) \frac{\partial^4 W}{\partial x^2 \partial y^2} - R_{24} \frac{\partial^4 W}{\partial y^4} - N_1 \frac{\partial^2 W}{\partial x^2} = 0 \end{aligned} \quad (13)$$

$$P_{22} \frac{\partial^4 F}{\partial x^4} + (P_{12} + P_{12} + P_{31}) \frac{\partial^4 F}{\partial x^2 \partial y^2} + P_{11} \frac{\partial^4 F}{\partial y^4} - P_{23} \frac{\partial^4 W}{\partial x^4} -$$

$$-(P_{13} + P_{24} - P_{32}) \frac{\partial^4 W}{\partial x^2 \partial y^2} - P_{14} \frac{\partial^4 W}{\partial y^4} = 0 \tag{14}$$

where R_{ij} and $P_{ij}(i, j = 1, 2, \dots, 4)$ denote parameters depending on the elastic properties of sandwich plates consisting of FG-nanocomposite layers.

4. Solution procedure

Since all edges of the sandwich plate are assumed to be simply supported, the solution of (13) and (14) is sought as follows [18, 19]:

$$W = f_1 \sin \frac{m\pi x}{a_1} \cos \frac{m\pi y}{a_2}, F = f_2 \sin \frac{m\pi x}{a_1} \cos \frac{m\pi y}{a_2} \tag{15}$$

where $f_i (i = 1, 2)$ denote unknown amplitudes, $m_i = \frac{m\pi}{a_i} (i = 1, 2)$ denote the wave parameters in which (m, n) is the wave mode.

Substituting (15) into the set of equations (14) and (13), then using Galerkin procedure and eliminating the unknown f_2 from the resulting equations and is considered f_1 to be nonzero, we obtain following expression for the dimensionless critical uniaxial compressive load sandwich plates consisting of the nanocomposite layers,

$$\begin{aligned} \bar{N}_1^{kr} = & \frac{1}{E_m^{(1)} h \beta_1^2} \{ [R_{13} \beta_1^4 + (R_{14} + 2R_{32} + R_{23}) \beta_1^2 \beta_2^2 + R_{24} \beta_2^4] - \\ & - [R_{12} \beta_1^4 + R_{21} \beta_2^4 + (R_{11} - 2R_{31} + R_{22}) \beta_1^2 \beta_2^2] \times \\ & \times \frac{P_{23} \beta_1^4 + (P_{13} - P_{32} + P_{24}) \beta_1^2 \beta_2^2 + P_{14} \beta_2^4}{P_{22} \beta_1^4 + (P_{12} + P_{31} + P_{21}) \beta_1^2 \beta_2^2 + P_{11} \beta_2^4} \} \end{aligned} \tag{16}$$

5. Results and discussion

In this subsection, the dimensionless uniaxial critical load values of sandwich plates consisting of homogeneous and heterogeneous nanocomposite layers with CNT welded $(0^\circ/90^\circ/0^\circ)$ and $(90^\circ/0^\circ/90^\circ)$ alignments are analyzed in comparison with single-layered plates with (0°) alignment. The properties of the nanocomposite consisting of single-walled CNT reinforced polymethyl methacrylate (PMMA) forming the layers of the sandwich plates are presented in table 1. Those data are taken from the study of Shen [7].

Elastic and geometric properties of CNT in the kth layer	Elastic and geometric properties of PMMA in the kth layer	Efficiency parameters of the nanocomposite in the kth layer
$E_{11cnt}^{(k)} = 5.6466 \times 10^{12} Pa,$ $E_{22cnt}^{(k)} = 7.08 \times 10^{12} Pa,$ $E_{12cnt}^{(k)} = 1.9445 \times 10^{12} Pa, \nu_{12cnt}^{(k)} = 0.175,$ $a_{1cnt} = 9.26 nm, r_{cnt} = 0.68 nm,$ $h_{cnt} = 0.067 nm$	$E_m^{(k)} = 2.5 \times 10^9 Pa,$ $\nu_m^{(k)} = 0.34$	$asV_{kn}^{*(k)} = 0.12; \eta_1^{(k)} = 0.137,$ $\eta_2^{(k)} = 1.022, \eta_3^{(k)} = 0.7\eta_2;$ $asV_{kn}^{*(k)} = 0.17; \eta_1 = 0.142,$ $\eta_2 = 1.626, \eta_3 = 0.7\eta_2;$ $asV_{kn}^{*(k)} = 0.28; \eta_1 = 0.141,$ $\eta_2 = 1.585, \eta_3^{(k)} = 0.7\eta_3$

Table 1. Properties of components forming nanocomposite in layers, and efficiency parameters

	$\bar{N}_1^{kr} \times 10^3$ (m, n) = (1,1)			
	U	V	O	X
a_1/h	$a_1/a_2 = 1, (0^\circ/90^\circ/0^\circ)$			
100	3.393	2.057	1.861	4.930
200	0.783	0.513	0.492	1.220
300	0.377	0.229	0.207	0.548
a_1/h	$a_1/a_2 = 2 (0^\circ/90^\circ/0^\circ)$			
100	7.003	5.675	6.224	7.829
200	1.844	1.412	1.613	2.119
300	0.778	0.631	0.692	0.870
a_1/h	$a_1/a_2 = 1 (0^\circ)$			
100	3.393	2.413	1.861	4.930
200	0.847	0.602	0.482	1.229
300	0.377	0.268	0.207	0.548
a_1/h	$a_1/a_2 = 2 (0^\circ)$			
100	5.314	4.382	3.694	6.982
200	1.332	1.112	0.891	1.732
300	0.590	0.487	0.410	0.776

Table 2. Distributions of \bar{N}_1^{kr} for (0°) single-layer and $(0^\circ/90^\circ/0^\circ)$ sandwich nanocomposite plates versus the a_1/h ratio for different a_1/a_2

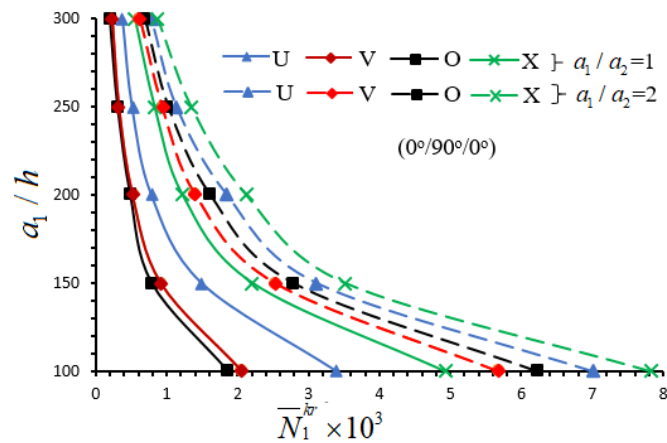


Figure 2. Distribution of dimensionless critical load values of sandwich plate with U, V, O and X pattern $(0^\circ/90^\circ/0^\circ)$ arrangement versus a_1/h for different a_1/a_2

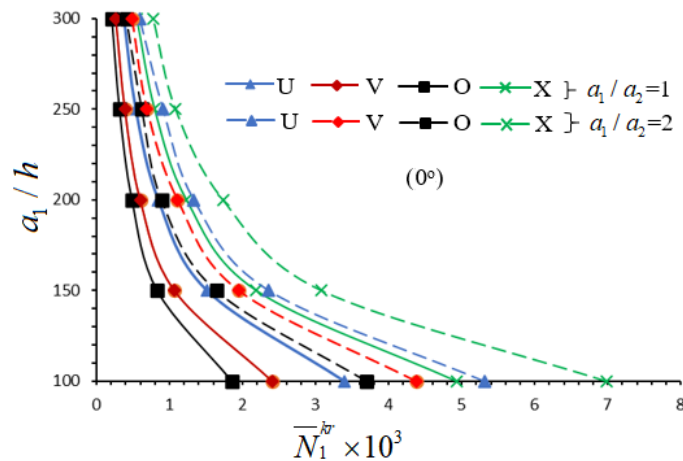


Figure 3. Distribution of dimensionless critical load values of (0°) single-layer plate with U, V, O and X patterns versus the a_1/h for different a_1/a_2 .

The distributions of the values of \bar{N}_1^{kr} for U, V, O and X patterned (0°) single-layer and sandwich nanocomposite plates with ($0^\circ/90^\circ/0^\circ$) alignment subjected to compressive uniaxial load in the Ox direction depending on the a_1/h for $\frac{a_1}{a_2} = 1$ and 2 are presented in table 2 and figures 2 and 3. As can be seen from table 2, when the a_1/h ratio increases, the critical load values decrease in all patterns of sandwich plates with ($0^\circ/90^\circ/0^\circ$) alignment and (0°) single-layer plates, while the values of the wave number remain constant. As can be seen from table 2 and figures 2 and 3, as the dimensionless critical compressive load values of the ($0^\circ/90^\circ/0^\circ$) arrangement sandwich plates with V, O and X patterns are compared with the dimensionless critical load values of the U patterned plate, the influences of V, O and X patterns change irregularly as the a_1/h ratio increases. For example, for $a_1/a_2 = 1$, the influences of V, O and X patterns on the critical load are 39.4%, 45.2% and (-45.3%), respectively, as $a_1/h = 100$, while those effects are 34.5%, 37.2% and (-55.8%), when $a_1/h = 200$ and 39.3%, 45.1% and (-45.2%), respectively, when $a_1/h = 300$. At $a_1/a_2 = 2$, the influences of V, O and X patterns on the critical load are 19%, 11.1%, and (-11.8%), respectively, as $a_1/h = 100$, while those effects are 23.4%, 12.5% and (-14.9%), when $a_1/h = 200$ and 18.9%, 11.1% and (-11.8%), respectively, when $a_1/h = 300$. When the critical load values of V, O and X patterned plates with ($0^\circ/90^\circ/0^\circ$) alignment are compared with the critical load values of the U patterned plate with ($0^\circ/90^\circ/0^\circ$) alignment, it is seen that the largest effect is in the X pattern and the smallest effect is in the O pattern.

When the critical load values of ($0^\circ/90^\circ/0^\circ$) arranged V, O and X patterned plates are compared with the critical load values of (0°) arranged patterned plates, when $a_1/h = 100$, the ratio difference between the critical load values is 10.49%, 0% and 0%, respectively. Those effects do not change in O and X, but decrease in V the pattern. It is seen that V, O, and X patterns are 10.35%, 0% and 0%, respectively. Therefore, sandwich plates reduce the critical load values compared to (0°) single layer plates.

6. Conclusion

In this study, the buckling of polymer-based sandwich rectangular plates with uniform and heterogeneous nanocomposite layers of CNT reinforcement subjected to uniaxial compressive loads is investigated. After construction of governing relations of sandwich plates consisting of polymer-based nanocomposite layers, the stability and strain compatibility equations are derived based on the assumptions of classical plate theory. Analytical expressions for the uniaxial critical compressive load are found for simply supported boundary conditions. Finally numerical calculations are made for the minimum values of the uniaxial critical compressive load for four different CNT patterns in the layers and various plate sizes and those calculations are interpreted.

Authors' Declaration

The authors declare no conflict of interests regarding the publication of this article.

References

1. S. Iijima, Nature **354** (1991) 56.
2. P. Ajayan, L. Schadler, P. Braun, Nanocomposite science and technology. Wiley-VCH Verlag GmbH & Co. KGaA (2003).
3. Y. Han, J. Elliott, Computational Materials Science **39** (2007) 315.
4. M. Kessler, W. Goertzen, Nanotechnology in Construction **3** (2009) 241.
5. K.M. Liew, Z.H. Pan, L.W. Zhang, Science China-Physics, Mechanics & Astronomy **63**(3) (2020) 234601.
6. H-S. Shen, Composite Structures **91**(1) (2009) 9.
7. H.-S. Shen, C.L. Zhang, Materials and Design **31**(7) (2010) 3403.
8. M. Mirzaei, Y. Kiani, Meccanica **51**(9) (2016) 2185.

9. A. Farzam, B. Hassani, *Composite Structures* **206** (2018) 774.
10. A. Sofiyev, U. Kaya, *UNEC Journal of Engineering and Applied Sciences* **2**(1) (2022) 19.
11. M. Avey, N. Fantuzi, A.H. Sofiyev, *Mathematics* **10**(7) (2022) 1081.
12. D. Zenkert, *An introduction to sandwich construction; Engineering materials advisory services (EMAS): London, UK; Stockholm, Sweden* (1995).
13. Z.X. Lei, L.W. Zhang, K.M. Liew, *Composite Structures* **152** (2016) 62.
14. V.T. Long, H.V. Tung, *Journal of Thermal Stresses* **42**(5) (2019) 658.
15. N. C. Tan, N. M. Dzung, N. H. Ha, N. D.Tien, N. C. Hung, A. H. Sofiyev, D. G. Ninh *AIAA Journal* **1** (2025) 1.
16. A.H. Sofiyev, M. Avey, *Mathematical Methods in the Applied Sciences* **9999** (2025) 1.
17. A.H. Sofiyev, M. Avey, N.M. Aslanova, *Mathematical and Computational Applications* **30** (1) (2025) 1.
18. M.R. Eslami, *Buckling and postbuckling of beams, plates and shells*. Springer, Switzerland (2018) 603 p.
19. J.N. Reddy, *Mechanics of laminated composite plates and shells: theory and analysis*. 2nd ed. CRC Press, New-York (2004) 858 p.